Electronic Supplementary Information for

Spectroscopic Mapping of the Gold Complex Oligomers (Dimer, Trimer, Tetramer, and Pentamer) by Excited-State Coherent Nuclear Wavepacket Motion in Aqueous Solutions

Munetaka Iwamura,[1]* Rina Urayama,[1] Airi Fukui,[1] Koichi Nozaki,[1] Li Liu,[2,3] Hikaru Kuramochi,[2,3] Satoshi Takeuchi[2,3] and Tahei Tahara[2,3]*

[1]Graduate School of Science and Engineering, University of Toyama, 3190 Gofuku, Toyama 930-8555, Japan

[2]Molecular Spectroscopy Laboratory, RIKEN, 2-1 Hirosawa, Wako, Saitama 351-0198, Japan

[3]Ultrafast Spectroscopy Research Team, RIKEN Center for Advanced Photonics (RAP), RIKEN, 2-1 Hirosawa, Wako, Saitama 351-0198, Japan

Contents

Section S1. Experimental

S1.1. Sample preparation

$K[Au(CN)_2]$ was purchased from Inuisho Precious Metals Co. (99.5% purity) or Tanaka Kikinzoku Kogyo Co. and recrystallized several times in water before use.

S1.2. Steady-state absorption and emission spectra

Absorption spectra were recorded using a commercial UV-visible absorption spectrometer (MPS-2000, Shimadzu, or V570DS JASCO with EHC 477T temperature controller) at 298 K. Sample solutions were put in quartz cells with 1-mm or 1-cm thickness, depending on the absorption intensities. Steady-state emission spectra were recorded using a commercial fluorometer (FP8500, JASCO) at 299 K. Sample solution was put in a quartz cell with 1-mm thickness, and the emission from the sample was collected with the front scattering geometry. The angle of incidence of the excitation light to the surface of the quartz cell was set at 60^o.

S1.3. Femtosecond time-resolved absorption measurements

The output from a Ti:sapphire regenerative amplifier system (Legend Elite, Coherent; 800 nm, 80 fs, 1 mJ, 1 kHz) was converted to ultraviolet pulses at 260 nm, 290 nm (Ex1), 310 nm (Ex2),[1] and 340 nm (Ex3) using an optical parametric amplifier (TOPAS−C, Light Conversion for the 260-, 290- and the 340 nm light; TOPAS, Quantronix for the 310 nm light) and subsequent frequency-quadrupling. The obtained ultraviolet pulses were used for photoexcitation. A small fraction of the 800 nm output of the regenerative amplifier was focused into a CaF_2 plate to generate a white-light continuum that covers a spectral range of 350 – 750 nm. It was used as the probe and reference pulses. The pump polarization was set at the magic angle with respect to the probe polarization. The sample solution was circulated through a fused-silica flow cell with a 0.5-mm path length. The probe and reference spectra of every five laser shots were measured with a spectrograph (500 is/sm, Chromex) equipped with a charge-coupled device (CCD) that was read out at a 100-Hz repetition rate (PIXIS 256E Princeton Instruments for the experiments with the 260-, 290- and the 340 nm light; TEA/CCD-1024-EM/1 UV, Princeton Instruments for the experiments with the 310 nm light). The effect of the chirp of the white-light probe on the time-resolved absorption spectra was corrected based on the optical Kerr effect (OKE) data of water, which were measured with exactly the same experimental configuration.[2] The full width at half maximum (FWHM) of the

instrumental response function (IRF) evaluated with the OKE measurement was 130 − 200 fs. All the measurements were performed at room temperature (299 K).

Steady-state absorption spectra of the sample solution were measured before and after the time-resolved measurements. No noticeable change was recognized, assuring that photo-degradation of the sample was negligible during the measurements.

S.1.4. Picosecond and nanosecond time-resolved emission measurements

Picosecond and nanosecond time-resolved emission measurements were carried out using a streak camera system (C4334, Hamamatsu). The measurements using excitation pulses at 290 (Ex1) and 340 nm (Ex3) were carried out using the laser system based on a Yb:KGW regenerative amplifier system (PHAROS, Light Conversion, 6 W, 6 kHz, 140 fs). The excitation pulses at 290 and 340 nm were generated by the second harmonic generation of the output from a home-built noncollinear optical parametric amplifier (NOPA) that was driven by the Yb:KGW regenerative amplifier. The measurement using excitation pulse at 310 nm (Ex2)[1] was performed using the laser system based on a Ti:sapphire regenerative amplifier system (Legend Elite, Coherent; 800 nm, 80 fs, 1 mJ, 1 kHz). The excitation pulse at 310 nm was generated by frequency-quadrupling of the output of an optical parametric amplifier (TOPAS, Light Conversion). In both cases, the sample was put in a cell with a thickness of 1 mm, and the emission was collected with the backscattering geometry. The pump polarization was set at the magic angle with respect to the detection polarization. Time-resolved traces were measured with the sweep ranges of 1 ~ 2000 ns. The shortest instrumental response time as good as 20 ps (FWHM) was obtained with the 1 ns sweep range. The spectral sensitivity of the streak camera system was corrected by using the steady-state emission spectra of the sample solution. All the measurements were performed at room temperature (296 K).

Section S2. Concentration dependence of the steady-state absorption spectra

Aqueous solutions of $K[Au(CN)_2]$ contain various oligomers such as the dimer, trimer, tetramer, and pentamer because they are in equilibrium in aqueous solutions. To estimate the excited-state species generated by photoexcitation, the information about the concentration-dependent change of the absorption spectrum is indispensable. Hence, steady-state absorption spectra of $K[Au(CN)_2]$ aqueous solutions were measured at various concentrations while keeping the ionic strength at μ = 1.0 mol/dm^3 by adding appropriate amounts of KCl into the solution. We stress that the measurements under the same ionic strength are critical for obtaining proper concentration dependence of the absorption spectrum (See ref.3, M. Iwamura et al, 2020, *Angew. Chem. Int. Ed*. 59, 23154, for more details). Figure S1 shows the absorption spectra obtained. Shoulder-like features appear in the wavelength region longer than 260 nm, and their intensity nonlinearly increases with the increase of the concentration (Figure S1a and S1b). As shown in Figure S1c, the absorbance at 266 nm is proportional to the square of the total concentration of $K[Au(CN)_2]$ (C), which is considered to indicate that the contribution of the dimer to the absorption at this wavelength is predominant, assuming that C is close to the concentration of the monomer. Thus, the dimer is expected to absorb most of the excitation light at ~270 nm. Absorbance at 290 nm is close to proportional to the square of C in the concentration region up to ~0.05 mol/dm^3, but it becomes close to the cube of C in the higher concentration region (Figure S1c), i.e. the intensity is reproduced by the sum of the square and the cube terms of the C. Thus, the absorption at 290 nm is considered to have contributions from both the dimer and trimer, which is consistent with the results of the frequency-wavelength 2D analysis (See main text). Absorbance at 310 nm and 340 nm is almost proportional to the cube of C (Figure S1b and S1c). This seems to suggest that absorbance around 310 – 340 nm is dominated by the trimer. In the case of the 310 nm excitation, the generation of the excited-state trimer was recognized by the excited-state vibration as well as time-resolved emission spectra (see main text and section S3). However, in the case of the 340 nm excitation to the 0.6-mol/dm^3 solution, our femtosecond time-resolved absorption data indicate that the excited species are dominated by the tetramer and pentamer, but the trimer is less contributed (see also main text). This implies that the total concentration is not close to the concentration of the monomer in solutions when large oligomers such as the pentamer are generated. Therefore, the concentration dependence of the absorption intensity at the excitation wavelength becomes inconclusive for identifying the excited species in the solutions of concentrations higher than ~0.1 mol/dm^3.

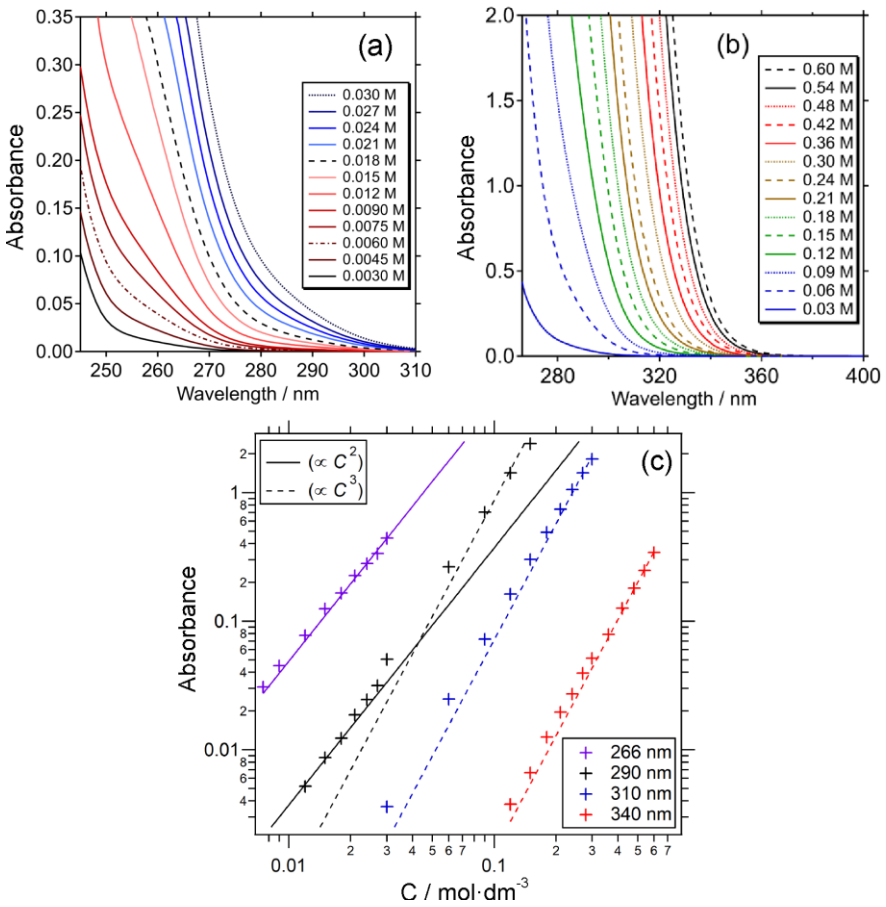

Figure S1. Steady-state absorption spectra of $K[Au(CN)_2]$ aqueous solutions at various concentrations at 298 K. (a, b) Absorption spectra of the concentration region from 0.003 – 0.03 mol/dm^3 (a) and 0.03 – 0.6 mol/dm^3 (b). (c) Concentration dependence of the absorbance at selected wavelengths measured with a 1-mm optical path length. The ionic strength is kept at μ = 1.0 mol/dm^3. Solid and dashed lines show the best fits proportional to the square and cube of the concentration, respectively.

Section S3. Steady-state and picosecond time-resolved emission spectra

We performed time-resolved emission measurements under the experimental conditions of Ex1 ([Au] = 0.080 mol/dm^3, λ_{ex} = 290 nm), Ex2 ([Au] = 0.28 mol/dm^3, λ_{ex} = 310 nm) and Ex3 ([Au] = 0.61 mol/dm^3, λ_{ex} = 340 nm) to confirm the excited-state species and their dynamics on the picosecond-nanosecond time scale. Because reliable assignments of the emission bands are indispensable for properly interpreting time-resolved emission data, we also carried out steady-state emission measurements.

S3.1. Concentration dependence of the steady-state emission spectra

Figure S2 shows the steady-state emission spectra of the $K[Au(CN)_2]$ solutions at various concentrations (0.0075 – 0.030 mol/dm^3), which were recorded with excitation at 266 nm under common ionic strength (μ = 1.0 mol/dm^3). Emission bands peaked at 330, 390, and 430 nm are recognized for all solutions. However, their relative intensities change as the increase of concentration and emission intensities. This indicates that the three emission bands originate from different oligomers, although absorbance at the excitation wavelength (266 nm) predominantly arises from the dimer. For making assignments of these three bands, we evaluated populations of the emitting species (C_n) generated by direct photoexcitation based on the dependence of the emission intensity on the total concentration of $K[Au(CN)_2]$ (C) using the following equation,

$$I_n(C) = \frac{\varepsilon_n C_n(C) d}{\sum_k \varepsilon_k C_k(C) d} a_n = \frac{\varepsilon_n C_n(C) d}{Abs_{ex}(C)} a_n \quad . \quad \text{(S1)}$$

Here, I_n, ε_n, and a_n are the quantities of the n-mer: the emission intensity per the absorbed photon number, the absorption coefficient at the excitation wavelength, and a parameter related to the emission yield, respectively.[3] Abs_{ex} and d are absorbance at the excitation wavelength and optical path length, respectively.[4] We ignored excited species generated by the diffusion processes such as a collision of excited n-mer and ground-state monomer to generate excited-state (n + 1)-mer. This assumption is adequate when the intrinsic emission lifetime of the n-mer is shorter than the time constant of the diffusion process, which is about ~10 ns under the present conditions.[1] Equation S1 can be rewritten as,

$$I_n(C) \cdot Abs_{ex}(C) = \varepsilon_n C_n(C) a_n d \quad . \quad \text{(S2)}$$

This equation shows that the product of $I_n(C) \cdot Abs_{ex}(C)$ is proportional to $C_n(C)$. We checked the total concentration (C) dependence of $I_n(C) \cdot Abs_{ex}(C)$ for the three emission bands, and the results as shown in Figure S2b. We found that the population of the species giving emission at

330 nm is proportional to C^2. Based on equation S2, this indicates that $C_n(C)$ is proportional to C^2, implying that the 330 nm emission band is assignable to the dimer. Similarly, $I_n(C) \cdot Abs_{ex}(C)$ for the 390 nm emission is proportional to C^3, indicating that the 390 nm emission is assignable to the trimer. These assignments are fully consistent with the assignments of the phosphorescence of the dimer and trimer in previous studies.[1, 5, 6] It is worth noting that the effect of the diffusion process on the emission intensities at 330 and 390 nm is negligible because the intrinsic lifetimes of the emission (28 ps and 1.4 ns, respectively, vide infra) are much shorter than the time constant of the diffusion process under these concentrations (longer than 10 ns).[1]

The quantitative analysis for the 430 nm emission band was not successful because the 430 nm emission heavily overlapped with the red side of the 390 nm emission band due to the trimer. Nevertheless, we can reasonably assign the 430 nm emission to an oligomer larger than the trimer because its intensity is lower than the 390 nm trimer emission when the concentration is lower than 0.02 mol/dm^3, but it becomes higher when the concentration is higher (Figure S1c). Hence, the 430 nm emission is assignable to the emission of the oligomer larger than the trimer, i.e., tetramer, being consistent with the assignments made in our previous paper.[6]

The emission bands at 330, 390 and 430 nm have been assigned to the phosphorescence of the dimer, trimer, and tetramer in our previous studies based on the analysis of the time-resolved emission and theoretical calculations.[3, 5, 6] We also reported very short S_1 lifetimes of the dimer, trimer and tetramer (0.2 ps, 0.5 ps, and 3 ps)[1, 6, 7] compared to the T_1 lifetimes (25 ps, 1.4 ns, and 23 ns, respectively, vide infra). Therefore, the steady-state emission spectra shown in Figure S2 are dominated by the phosphorescence of the dimer, trimer, and tetramer. This assignment is confirmed by the results of the time-resolved emission measurements that are described in the next section.

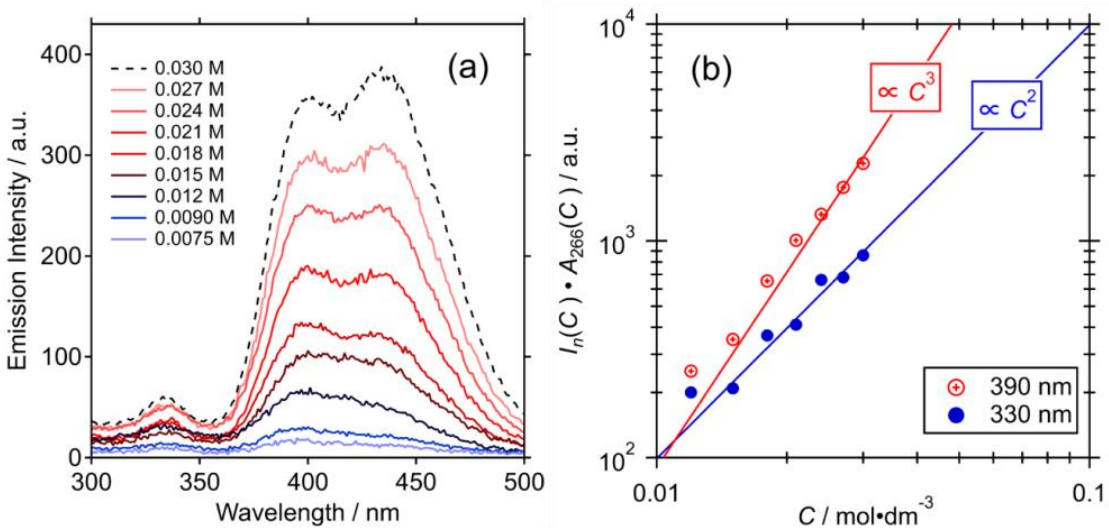

Figure S2. Steady-state emission of $K[Au(CN)_2]$ solutions with different concentrations. (a) Emission spectra measured at 299 K with excitation at 266 nm. (b) Product of emission intensity ($I_n(C)$) and absorption intensity at 266 nm ($A_{266}(C)$) plotted against the total concentration of $K[Au(CN)_2]$ (C). The ionic strength of the solutions was kept at μ = 1.0 mol/dm^3 by the addition of KCl.

S3.2. Picosecond and nanosecond time-resolved emission spectra

Picosecond and nanosecond time-resolved emission spectra of the $K[Au(CN)_2]$ aqueous solutions were measured under the three experimental conditions of Ex1, Ex2, and Ex3. As described below, the obtained data clarified the excited-state oligomers that predominantly contribute to the emission under the three conditions: the dimer and the trimer (Ex1), the trimer and the tetramer (Ex2), and the pentamer (Ex3).

S3.2.1. Ex1 ([Au] = 0.080 mol/dm^3, λ_{ex} = 290 nm)

Figure S3a shows time-resolved emission spectra measured under Ex1. Immediately after photoexcitation, the emission bands peaked at 350 nm and 400 nm are observed. Then, the 350 nm emission band quickly disappears (within the time-resolution of the streak camera; < 20 ps), but the 400 nm emission remains. In the time-resolved spectrum at 0.0 ns, these two emission bands appear with comparable intensities. However, the intrinsic intensity of the 350 nm emission is considered to be much higher than that of the 400 nm emission because the lifetime of the 350 nm emission is much shorter than the time resolution of the measurement. Therefore, the 350 nm emission is assignable to the fluorescence of the initially excited oligomers, whereas the 400 nm emission is attributed to the phosphorescence from the triplet oligomer generated by the intersystem crossing. In addition to the main phosphorescence band peaked at 400 nm, the time-resolved emission spectrum at 0.05 ns exhibits a small band peaked at 330 nm. Furthermore, the temporal evolution of the emission spectrum in the time region of 0.5 – 4.7 ns reveals that there is another longer-lived phosphorescence band peaked at 430 nm. Consequently, in addition to the fluorescence band peaked at 350 nm, we see three phosphorescence bands showing different peak wavelengths (350, 400, and 430 nm) and distinct lifetimes under Ex1. Based on the analysis of the steady-state emission spectra described in S3.1, these phosphorescence bands are attributed to the T_1 dimer (330 nm), T_1 trimer (400 nm), and T_1 tetramer (430 nm). The fluorescence band at 350 nm is assignable to the emission from the S_1 trimer because the phosphorescence in the early time region is dominated by the trimer. This assignment is consistent with our previous fluorescence up-conversion measurements, which showed that the fluorescence of the S_1 trimer appears at around 350 nm with a lifetime of 0.38 ps.[7]

The phosphorescence of the dimer (330 nm emission) decays with a time constant of 28 ps (Figure S3a-3 inset), which accords well with the lifetime of the T_1 dimer determined in our previous time-resolved absorption and emission measurements for 0.038 mod/dm^3 solution performed with excitation at 266 nm.[6] Emission at 400 nm decays with a time constant of 1.4 ns, while its red shoulder (430 nm) shows a slight intensity increase with the same time constant of 1.4 ns. This dynamics is attributable to the decay of the T_1 trimer phosphorescence and the

concomitant rise of the T_1 tetramer phosphorescence. Their same time constants indicate that some T_1 tetramer is generated from the T_1 trimer by a collision between the T_1 trimer and a ground-state monomer. It is worth noting that a similar decay time (1.6 ns) of the T_1 trimer phosphorescence was observed for the solution of 0.038 mol/dm^3, which is a much more diluted condition.[6] Because the decay of the T_1 trimer phosphorescence is not sensitive to the concentration, we can safely consider that the lifetime of the T_1 trimer is mainly determined by the intrinsic lifetime of the T_1 trimer and that only a small amount of T_1 tetramer is generated from the T_1 trimer by the collision process. Thus, the yield of the T_1 tetramer formation from the T_1 trimer is expected to be small under the condition of Ex1. The 430 nm emission decays with a time constant of 23 ns. This is the intrinsic lifetime of the T_1 tetramer.[1, 8]

S3.2.2. Ex2 ([Au] = 0.28 mol/dm^3, λ_{ex} = 310 nm)

Figure S3b shows time-resolved emission data taken under Ex2, for which original data were already reported in our previous work.[1] Immediately after photoexcitation, short-lived emission is observed. The peak of this emission was located in the wavelength region shorter than 400 nm, and its lifetime is shorter than the time resolution of the streak camera (< 20 ps). After the decay of the initial emission, an emission peaked at ~400 nm was observed with a much lower intensity than that of the initial short-lived emission. The initial emission is assigned to the fluorescence, and the following weak emission is to the phosphorescence of initially excited species. In our first paper[1], we assigned this phosphorescence band solely to the T_1 trimer. However, our later TR-ISRS study[7] and the excited-state nuclear motion detected in this study show that the excited species generated under Ex2 are not only the trimer but also the tetramer. Actually, the emission spectrum at 0.4 ns exhibits a tail extending toward 500 nm (Figure S3b-1), implying that this phosphorescence band contains the contribution from the phosphorescence of the T_1 tetramer.

The decay of the phosphorescence peaked at ~400 nm and the rise of another emission peaked at 460 nm were observed with a time constant of 2 ns. This dynamics is attributed to the formation of a larger oligomer from the T_1 trimer and T_1 tetramer by the collision with a ground-state monomer. The peak of this new emission (460 nm) is longer than the peak of the phosphorescence of the T_1 tetramer (430 nm), indicating that this emission arises from an oligomer larger than a tetramer (i.e., pentamer). This 460 nm emission decays with a time constant of 13 ns, indicating that 13 ns is the lifetime of the T_1 pentamer.

S3.2.3. Ex3 ([Au] = 0.61 mol/dm^3, λ_{ex} = 340 nm)

Figure S3c shows time-resolved emission data taken under Ex3. Immediately after the photoexcitation, short-lived emission is observed at ~430 nm (Figure S3c-1). The decay of this

emission is dominated by an exponential decay with a time constant of 13 ps (Figure S3c-2). After this 13 ps decay, weak emission peaked at 460 nm is observed at 0.26 ns, which exhibits a slight redshift from 460 to 470 nm with a time constant of 0.6 ns. This redshift is more readily seen as the decay of the emission on the short-wavelength side and the rise on the long-wavelength side (Figure S3c-3). The resultant 470 nm emission decays with a time constant of 15 ns.

The initial bright, short-lived emission is assignable to the fluorescence from initially excited species. Because the later phosphorescence appears at the wavelength (460 nm), which is longer than the phosphorescence of the T_1 tetramer (430 nm), the excited species that is predominantly generated under Ex3 is a larger oligomer such as the pentamer. (We note that the excited-state nuclear motion detected in this study indicates that the excited-state tetramer is also generated under this condition.) Therefore, the first short-lived emission showing the 13 ps decay is attributed to the S_1 pentamer, which yields the T_1 pentamer exhibiting phosphorescence at 460 nm. The following redshift of the T_1 pentamer phosphorescence from 460 nm to 470 nm is attributable to the generation of the T_1 state of larger oligomers, such as T_1 hexamer, by the collision with a ground-state monomer, as observed for smaller T_1 oligomers under Ex1 and Ex2. The time constant (0.6 ns) for this collision process under Ex3 is much shorter than those under Ex1 and Ex2 (~ 2 ns), which is due to more frequent collisions occurring under a higher concentration condition of Ex3. The yield of the larger T_1 oligomers (e.g. the T_1 hexamer) by this collision process may be as high as unity under Ex3, because the emission intensity at 460 nm due to T_1 pentamer at 0.26 ns is close to that of T_1 hexamer at 470 nm at ~ 2 ns (Figure S3c-1).

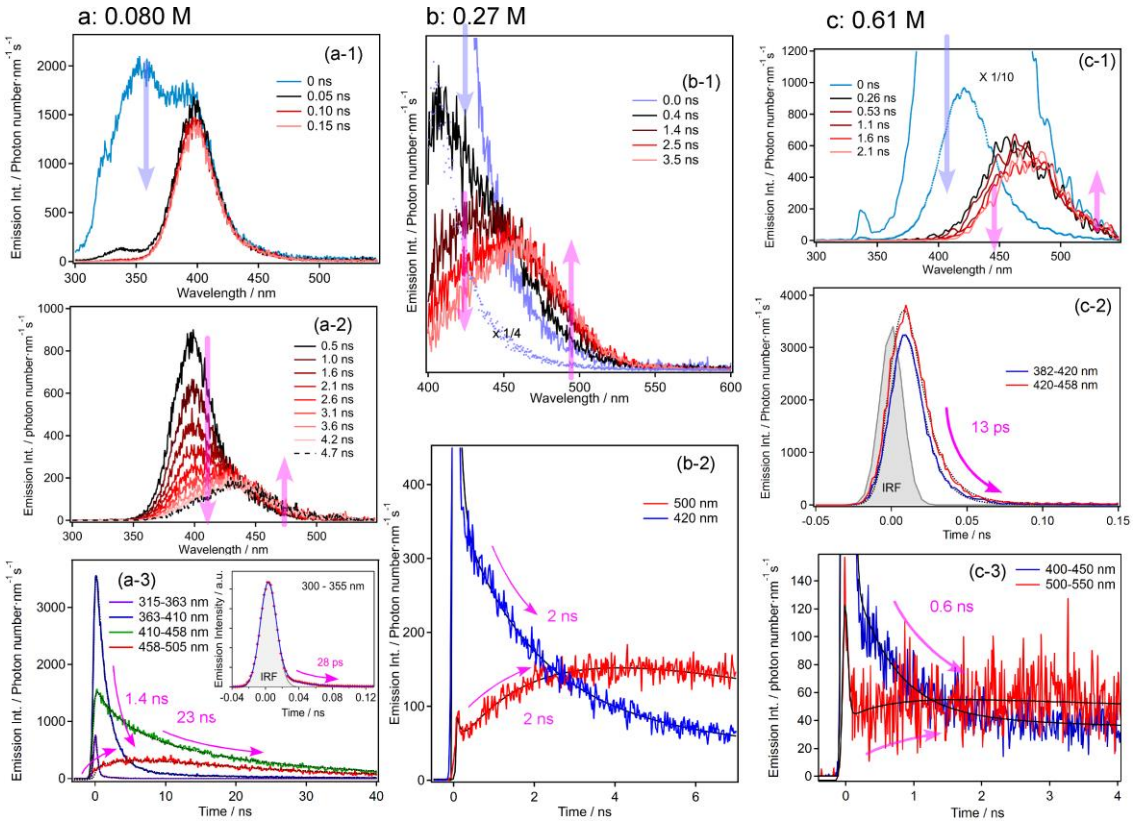

Figure S3. Time-resolved emission data of $K[Au(CN)_2]$ aqueous solutions. (a) Data under Ex1 ([Au] = 0.080 mol/dm^3, λ_{ex} = 290 nm). Time-resolved emission spectra for 0 – 0.15 ns (a-1) and (a-2), and the temporal profiles in the delay time ranges of -3 – 40 ns (a-3) and -0.04 – 0.12 ns (a-3 inset). (b) Data under Ex2 ([Au] = 0.27 mol/dm^3, λ_{ex} = 310 nm). Time-resolved emission spectra for 0 – 3.5 ns (b-1) and the temporal profiles in the delay time range of -0.5 – 7 ns (b-2). (c) Data under Ex3 ([Au] = 0.61 mol/dm^3, λ_{ex} = 340 nm). Time-resolved emission spectra for 0 – 2.1 ns (c-1). Temporal profiles in the delay time regions of -0.05 – 0.15 ns (c-2) and -0.3 – 4 ns (c-3). The data in Figure S3b has been published in our previous paper.[1] Reprinted with permission from *J. Am. Chem. Soc*., 2013, 135, 538-541. Copyright [2013] American Chemical Society.

Section S4. Kinetic analysis for time-resolved absorption spectra

As described in the main text, femtosecond time-resolved absorption spectra were measured under the three experimental conditions of Ex1, Ex2, and Ex3, and the peak wavelengths of the transient absorption of excited-state oligomers were determined by the frequency–wavelength 2D analysis. In this section, we describe the details of the temporal changes of time-resolved absorption spectra and the results of the fitting analysis of their temporal profiles.

S4.1. Ex1 ([Au] = 0.080 mol/dm^3, λ_{ex} = 290 nm)

Under Ex1, the excited-state dimer and trimer are predominantly generated, as concluded by the frequency–wavelength 2D analysis (See main text) and the time-resolved emission experiments (Section S3). Femtosecond time-resolved absorption spectra taken under Ex1 are shown in Figure 2a (main text). Immediately after photoexcitation, a broad absorption band peaked at ~550 nm appears. A rise of the transient absorption in the whole wavelength region (370 – 750 nm) is observed in the time region earlier than 1 ps. Then, up to 5 ps, a slight rise at ~550 nm and slight decay at ~670 nm are observed (Figure 2a-2), which is followed by a substantial decay of the broad transient band continuing up to 250 ps (Figure 2a-3). In the 250 – 500 ps time region, a small red shift of the transient absorption peaked at 550 nm is recognized.

The above-described spectral changes of the transient absorption are well reproduced by five time constants of 0.2 ps (the initial rise in the whole region of 370 – 750 nm), 2.1 ps (rise at 550 nm and decay at 670 nm), 25 ps (decay of the broad band in the 400 – 700 nm region), 2 ns (decay around 550 nm and rise around 600 nm) and very long one, which are obtained by the global fitting analysis using a multi-exponential function (see Figure S4 and S5 for the fitting results and relevant decay associated spectra, respectively). As mentioned in the main text, the 0.2 ps component is attributed to the $S_1 \rightarrow T_1$ intersystem crossing in the dimer and the trimer. The 2.1 ps spectral change is due to the bent-to-linear structural change of the T_1 trimer. The 25 ps time constant is the lifetime of the T_1 dimer. The 2 ns spectral change giving rise to a decay at ~550 nm and a rise at ~600 nm is assignable to the generation of the T_1 tetramer from the T_1 trimer through collision with a ground-state monomer, because this 2 ns time constant agrees well with the time constant assigned to this process in the time-resolved emission data (Section S3 in ESI). We note that the decay-associated spectrum of the 2.1 ps time constant shows a negative band at ~550 nm, indicating the rise of a band peaked at this wavelength. This peak wavelength well matches the peak of the transient absorption of the T_1 trimer determined by the frequency−wavelength 2D plots (550 nm, Table 1).[6, 9]

S4.2. Ex2 ([Au] = 0.28 mol/dm^3, λ_{ex} = 310 nm)

Under Ex2, the excited-state trimer and tetramer are predominantly generated by photoexcitation, as concluded by the frequency–wavelength 2D analysis (main text) and the time-resolved emission experiments (Section S3 in ESI). Femtosecond time-resolved absorption spectra taken under Ex2 are shown in Figure 2b (main text). The rise of a transient absorption band at ~ 600 nm is observed in the time region from 0 to 60 ps.

The spectral change up to 60 ps are well reproduced by three time constants of 0.24 ps (initial rise at 625 nm), 2.1 ps (rise at 575 nm), and very long one,[1] The fitting results are shown in SI of the literature[1] and relevant decay associated spectra are shown in Figure S6. As mentioned in the main text, the 0.24 ps rise is attributed to the $S_1 \rightarrow T_1$ intersystem crossing of the trimer. There are two processes that are assignable to the ~2 ps spectral change, which is the bent-to-liner structural change of the T_1 trimer and the $S_1 \rightarrow T_1$ intersystem crossing of the tetramer. Because the time constants of these two processes are similar to each other, they provide one single time constant in the analysis.

S4.3. Ex3 ([Au] = 0.61 mol/dm^3, λ_{ex} = 340 nm)

Under Ex3, the excited-state tetramer and pentamer are mainly generated, as shown by the frequency-wavelength 2D analysis. In addition, the time-resolved emission experiments indicate that the excited-state pentamer highly likely has a larger population than the excited-state tetramer under this experimental condition although radiative rate constants of the tetramer and the pentamer are unknown. Femtosecond time-resolved absorption spectra taken under Ex3 are shown in Figure 2c (main text). Immediately after photoexcitation, a transient absorption band peaked at ~620 nm is observed (Figure 2c-1). This transient absorption band continues to rise up to 500 ps with a red shift in the time region later than ~10 ps (Figure 2c-2).

The above-described spectral changes of the transient absorption are well reproduced by five time constants of 1 ps (rise at ~620 nm), 10 ps (rise at ~ 650 nm), 0.1 ns (decay at ~580 nm), 0.6 ns (rise at ~ 700 nm), and a very long one (see Figure S7 for the fitting results and Figure S8 for the decay-associated spectra). Because the fluorescence lifetimes of the S_1 tetramer and S_1 pentamer are 3 ps[7] and 10 ps (see section S3), respectively, the 1 and 10 ps components are assignable to the $S_1 \rightarrow T_1$ intersystem crossing in the tetramer and the pentamer, respectively. The 0.1 ns decay and 0.6 ns rise components reflect a redshift of the transient absorption peak from ~620 nm to ~670 nm. Although the time constants of the decay and rise are somewhat different from each other, we consider that these time constants represent the conversion processes from initially excited oligomers to larger ones (i.e., from pentamer to hexamer) by the collision with a ground-state monomer because this process is recognized in the time-resolved emission data in

the same time region. A long-lived absorption band is assignable to large oligomers such as T_1 hexamer.

S4.4. Analysis of temporal profiles of time-resolved absorption.

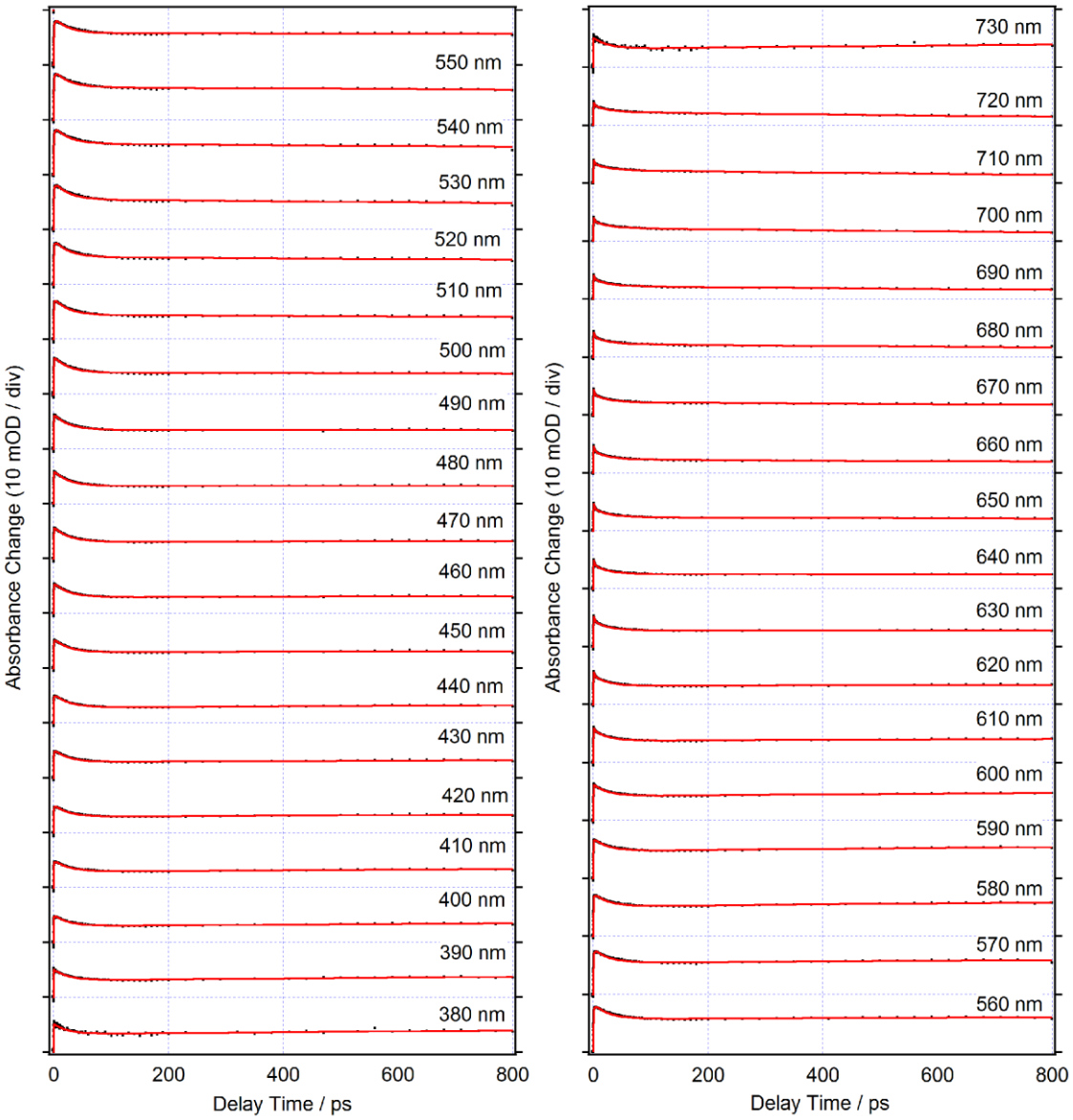

Figure S4. Temporal profiles of the femtosecond time-resolved absorption signal of $K[Au(CN)_2]$ in an aqueous solution in the wavelength range of 380 − 730 nm at the delay time of -0.05 – 800 ps (Ex1: [Au] = 0.080 mol/dm^3, λ_{ex} = 290 nm). A global fitting analysis was carried out using the sum of four exponential functions, and the best fits (red curves) were obtained with the time constants of 0.2 ps, 2.1 ps, 25 ps, 2 ns, and a very long one (23 ns).

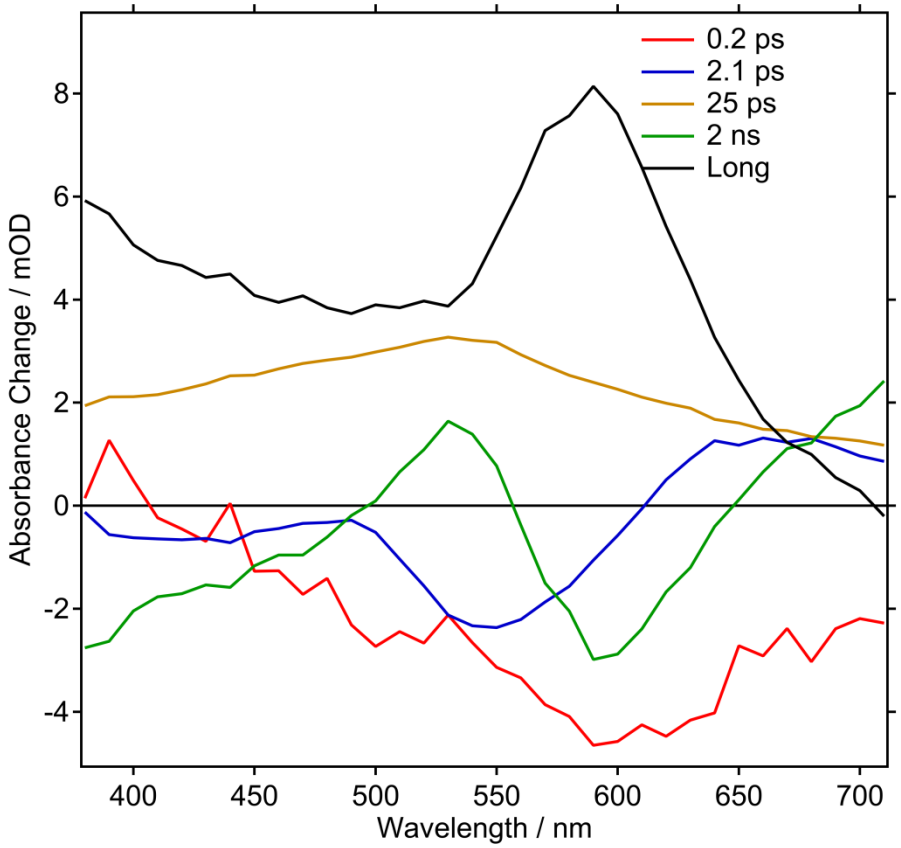

Figure S5. Decay-associated spectra obtained from the femtosecond time-resolved absorption data of $K[Au(CN)_2]$ in an aqueous solution, which correspond to the pre-exponential factors of each exponential function of the best fits to the temporal profiles shown in Figure S4. (Ex1: [Au] = 0.080 mol/dm^3, λ_{ex} = 290 nm).

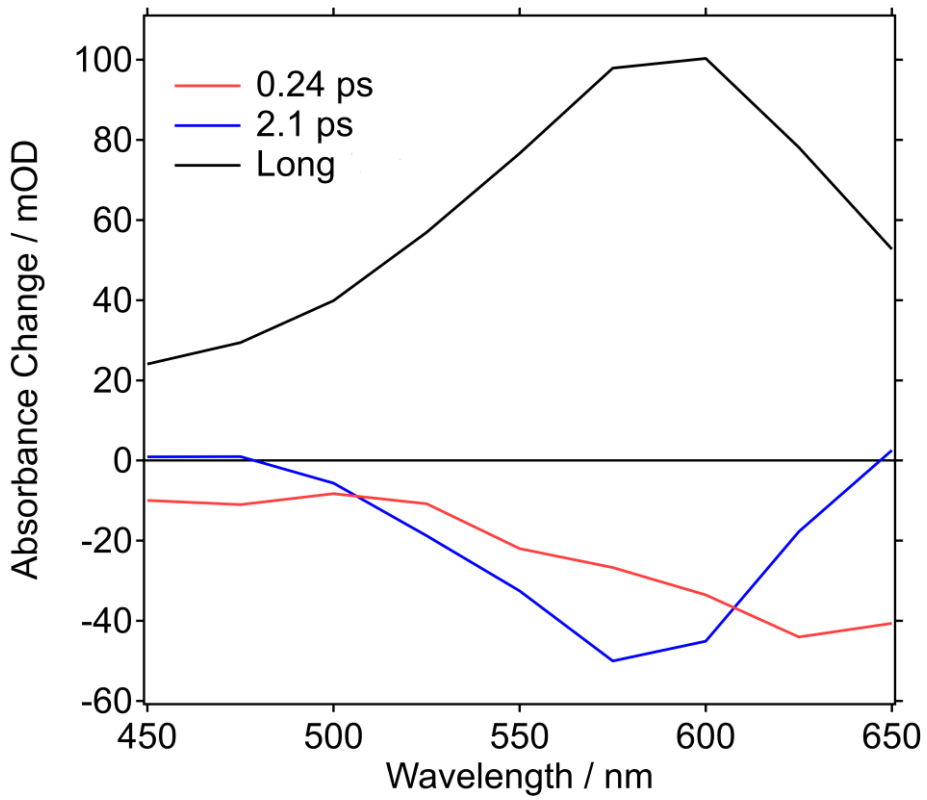

Figure S6. Decay-associated spectra obtained from the femtosecond time-resolved absorption data of $K[Au(CN)_2]$ in an aqueous solution, which correspond to the pre-exponential factors of each exponential function of the best fits to the temporal profiles shown in Figure S3 in SI of our previous paper.[1] (Ex2. [Au] = 0.28 mol/dm^3, λ_{ex} = 310 nm).

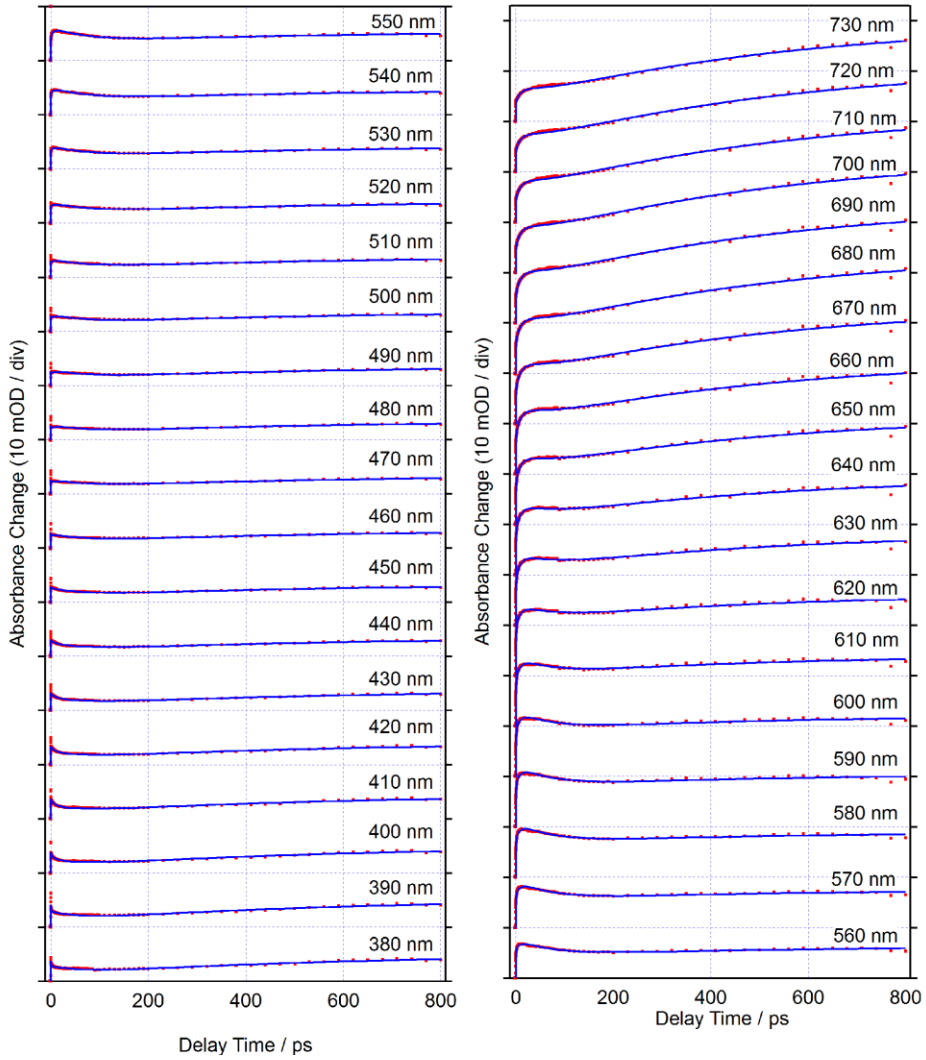

Figure S7. Temporal profiles of the femtosecond time-resolved absorption signal of $K[Au(CN)_2]$ in an aqueous solution in the wavelength range of 380 − 730 nm at the delay time of -0.05 – 800 ps (Ex3: [Au] = 0.61 mol/dm^3, λ_{ex} = 340 nm). A global fitting analysis was carried out using the sum of four exponential functions, and the best fits (red curves) were obtained with the time-constants of 1 ps, 10 ps, 0.1 ns, 0.6 ns and a very long one (13 ns).

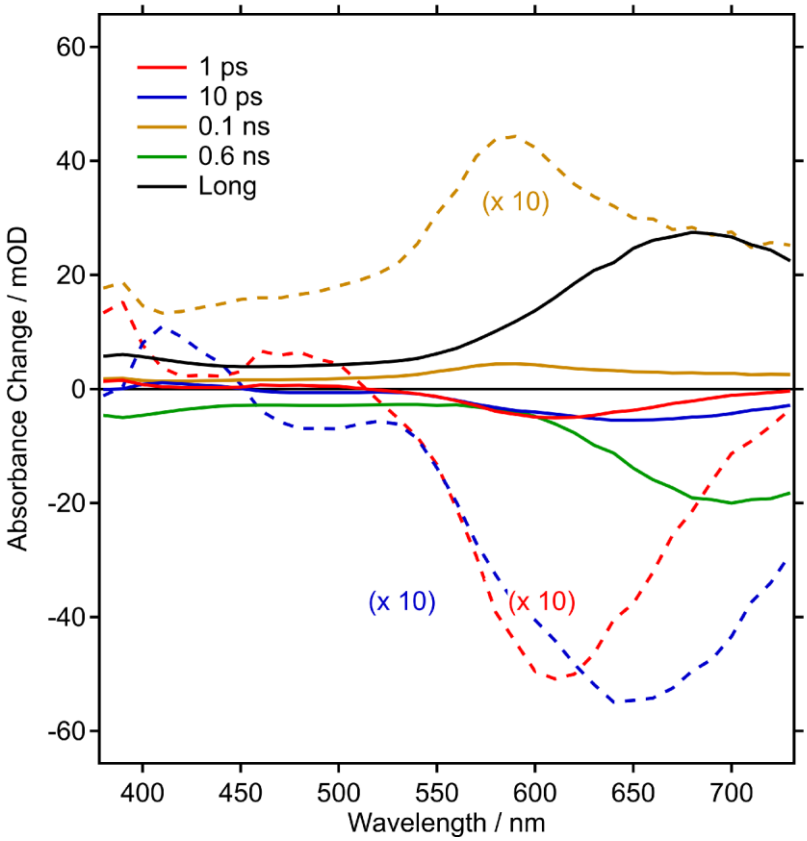

Figure S8. Decay-associated spectra obtained from the femtosecond time-resolved absorption data of $K[Au(CN)_2]$ in an aqueous solution, which correspond to the pre-exponential factors of each exponential function of the best fits to the temporal profiles shown in Figure S7. (Ex3: [Au] = 0.61 mol/dm^3, λ_{ex} = 340 nm).

S4.5. Comparison of the results of the femtosecond time-resolved absorption experiments and analysis under Ex1, Ex2, and Ex3

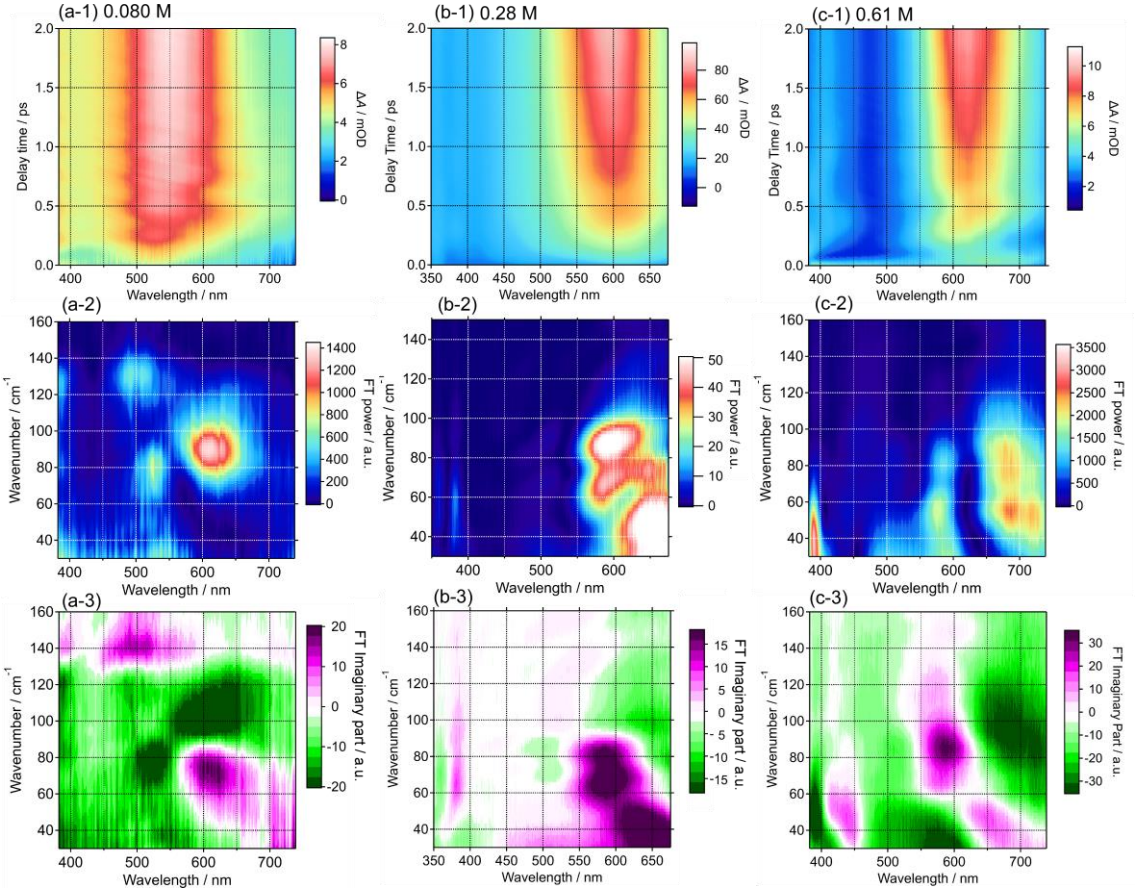

Figure S9. Femtosecond time-resolved absorption data and analysis of $K[Au(CN)_2]$ aqueous solution. 2D plot of femtosecond time-resolved absorption data (a-1, b-1, c-1), and Frequency–wavelength 2D plots of the power spectra (a-2, b-2, c-2) and the imaginary part amplitude (a-3, b-3, c-3) of the Fourier transform. (a: Ex1, [Au] = 0.080 mol/dm^3, λ_{ex} = 290 nm; b: Ex2, [Au] = 0.28 mol/dm^3, λ_{ex} = 310 nm; c: Ex3, [Au] = 0.61 mol/dm^3, λ_{ex} = 340 nm.) The frequency-wavelength 2D plots of the real part amplitude of the Fourier transform are shown in Figure 3 of the main text. The data shown in Figure S9b has been published in our previous paper[1].

S5. Time-resolved absorption spectra of $K[Au(CN)_2]$ aqueous solution of 0.30 mol/dm^3, λ_{ex} = 260 nm.

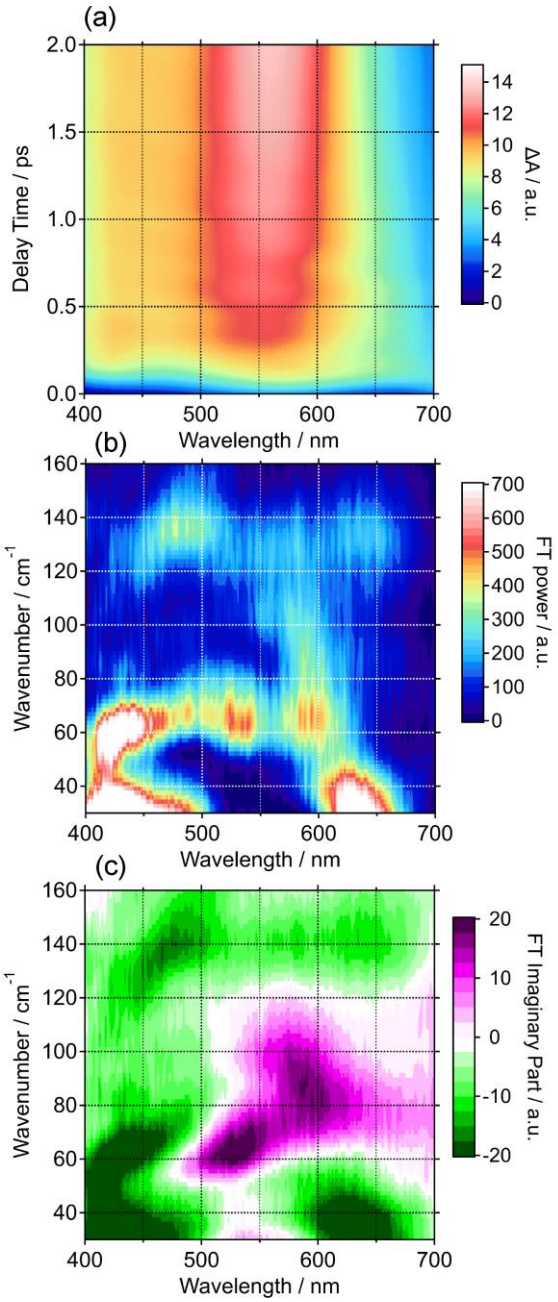

Figure S10. Femtosecond time-resolved absorption data and analysis of $K[Au(CN)_2]$ aqueous solution. 2D plot for the time-resolved absorption spectra (a), the Frequency–wavelength 2D plot of the power spectra (b) and the imaginary part amplitude (c) of the Fourier transform. The Frequency–wavelength 2D plot of the real part amplitude of the Fourier transform is shown in the main text. ([Au] = 0.30 mol/dm^3, λ_{ex} = 260 nm)

References

1. M. Iwamura, K. Nozaki, S. Takeuchi and T. Tahara, *J. Am. Chem. Soc.*, 2013, 135, 538-541.
2. S. Yamaguchi and H. Hamaguchi, *Appl. Spect.*, 1995, 49, 1381-1542.
3. M. Iwamura, A. Fukui, K. Nozaki, H. Kuramochi, S. Takeuchi and T. Tahara, *Angew. Chem. Int. Ed.*, 2020.
4. The optical path in the solution is 1 mm though the incident angle of the excitation light is 60^{o}. Since the excitation light is refracted at the surfece, it becomes almost 90^{o} from the optical surface in the sample solution. This was confirmed by measuring the absorbance of the sample solution in the 1-mm cell with the 60^{o} setup.
5. M. A. Rawashdeh-Omary, M. A. Omary, H. H. Patterson and J. John P. Fackler, *J. Am. Chem. Soc.*, 2001, 123, 11237-11247.
6. M. Iwamura, R. Wakabayashi, J. Maeba, K. Nozaki, S. Takeuchi and T. Tahara, *Phys. Chem. Chem. Phys.*, 2016, 18, 5103-5107.
7. H. Kuramochi, S. Takeuchi, M. Iwamura, K. Nozaki and T. Tahara, *J. Am. Chem. Soc.*, 2019, 141, 19296-19303.
8. R. Wakabayashi, J. Maeba, K. Nozaki and M. Iwamura, *Inorg. Chem.*, 2016, 55, 7739-7746.
9. M. Iwamura, K. Kimoto, K. Nozaki, H. Kuramochi, S. Takeuchi and T. Tahara, *J. Phys. Chem. Lett.*, 2018, 9, 7085-7089.